



## Energy interval 3S-1S in muonic hydrogen

A. E. Dorokhov *Joint Institute of Nuclear Research, BLTP, 141980, Moscow region, Dubna, Russia*

R. N. Faustov

*Institute of Cybernetics and Informatics in Education, FRC CSC RAS, Moscow, Russia*A. P. Martynenko  and F. A. Martynenko *Samara National Research University, Moskovskoye Shosse 34, 443086, Samara, Russia*

(Received 18 October 2020; accepted 7 December 2020; published 23 December 2020)

The energy interval (3S-1S) in muonic hydrogen is calculated on the basis of quasipotential approach in quantum electrodynamics. We take into account different corrections of orders  $\alpha^3$ – $\alpha^6$ , which are determined by relativistic effects, the effects of vacuum polarization, nuclear structure, and recoil, as well as combined corrections including the above. Nuclear structure effects are expressed in terms of the charge radius of the proton in the case of one-photon interaction and the proton electromagnetic form factors in the case of two-photon exchange interaction. The value of the energy interval (3S-1S) can be used for a comparison with future experimental data and determining the proton charge radius with greater accuracy.

DOI: [10.1103/PhysRevA.102.062820](https://doi.org/10.1103/PhysRevA.102.062820)

### I. INTRODUCTION

At present, four complementary methods are used to obtain the charge radii of light nuclei: elastic scattering of electrons on nuclei, elastic scattering of muons on nuclei, spectroscopy of electron atoms, and high-precision laser spectroscopy in muonic atoms [1–4]. Traditionally, elastic electron scattering was the first method to determine internal structure of nuclei. Elastic scattering of leptons by a nucleus target is described by form factors included in the theoretical expression for the scattering cross section. A proton or other light nucleus is a compound particle, and its size is determined by the charge radius  $r_p$ . It is related to the slope of the electric form factor of the proton  $G_E$  at  $q^2 = 0$ . Since  $G_E$  is a nonperturbative function of  $q^2$ , its slope should be extracted from experimental data. The most direct way to measure  $r_p$  is to extract the electric form factor  $G_E$  from lepton-proton scattering and determine its slope at  $q^2 = 0$ . Experimental data provide detailed information on the distribution of electric charge and magnetic moment inside the proton. They are used to determine the absolute values of the proton charge  $r_p$  and magnetic  $r_M$  radii, usually with a percentage accuracy or slightly better. At present, experiments are being carried out on the scattering of electrons and muons by protons. By simultaneously determining the form factors for electron and muon scattering, these experiments will allow an accurate test of the universality of the lepton, thus contributing to the solution of the “puzzle” with the proton radius in the near future [5,6].

Atomic spectroscopy of hydrogen is an indirect way of determining the charge radius  $r_p$  of a proton from precision measurements of certain energy intervals. While electron scattering and spectroscopy of electron atoms were available for

a long time, muon spectroscopy became available only in 2010 due to the work of the CREMA collaboration. As a result of the first CREMA experiments that year, the value  $r_p = 0.84184(67)$  fm was obtained, which was 10 times more accurate than all previous values from experiments with electronic systems. Moreover, this value was significantly less than the CODATA value,  $r_p = 0.8768(69)$  fm. This difference is called the “puzzle” of the proton radius. It is safe to say that the past decade has been CREMA’s decade. Let us list the main experimental results obtained during this time and published:

(1) The measurement of transition frequency ( $2S_{1/2}^{F=1} - 2P_{3/2}^{F=2}$ ) in muonic hydrogen in 2010 [7].

(2) The measurement of two transition frequencies ( $2S_{1/2}^{F=1} - 2P_{3/2}^{F=2}$ ) and ( $2S_{1/2}^{F=0} - 2P_{3/2}^{F=1}$ ) in muonic hydrogen and the measurement of hyperfine structure of the 2S state in 2013 [8,9].

(3) The measurement of three transition frequencies between energy levels 2P and 2S in muonic deuterium: ( $2S_{1/2}^{F=3/2} - 2P_{3/2}^{F=5/2}$ ), ( $2S_{1/2}^{F=1/2} - 2P_{3/2}^{F=3/2}$ ), ( $2S_{1/2}^{F=1/2} - 2P_{3/2}^{F=1/2}$ ) [10].

The performed studies with muonic hydrogen showed that there is a significant discrepancy in the values of the charge radius of the proton and deuteron, which are obtained from experiments with electronic and muonic atoms. In the case of other light nuclei (helium), the results are preliminary and have so far been reported only at conferences.

During 2017–2019 different experimental results were obtained, with both electronic and muonic systems, which made it possible to extract the value of the charge radius of the proton. In Ref. [11] the frequency of the

TABLE I. Corrections to energy interval (3S-1S) in muonic hydrogen.

No.	Contribution to the interval (3S-1S)	( $\mu p$ ), meV
1	Fine structure correction (1)	2 247 582.5823
2	Vacuum polarization correction in $1\gamma$ interaction of order $\alpha(Z\alpha)^2$	1834.5535
3	Muon VP correction in $1\gamma$ interaction of order $\alpha(Z\alpha)^4$	0.1276
4	Wichman-Kroll correction	-0.0110
5	Light-by-light correction	0.0044
6	Two-loop VP correction in $1\gamma$ interaction of order $\alpha^2(Z\alpha)^2$	12.8432
7	Three-loop VP correction in $1\gamma$ interaction of order $\alpha^3(Z\alpha)^2$	0.0246
8	Relativistic corrections with the account of one-loop VP in FOPT	-0.1804
9	Relativistic corrections with the account of two-loop VP in FOPT	-0.0010
10	Relativistic corrections with the account of one-loop VP in SOPT	0.2900
11	Relativistic corrections with the account of two-loop VP in SOPT	-0.0012
12	Two-loop VP correction in second-order PT of order $\alpha^2(Z\alpha)^2$	1.9955
13	Three-loop VP correction in second-order PT of order $\alpha^3(Z\alpha)^2$	0.0294
14	Three-loop VP correction in third-order PT of order $\alpha^3(Z\alpha)^2$	0.0032
15	Nuclear structure correction of order $(Z\alpha)^4$	$-28.31 \pm 0.04$
16	Correction to the nuclear structure with the account of vacuum polarization of order $\alpha(Z\alpha)^4$	-0.1705
17	Correction to the nuclear structure with two-loop VP of order $\alpha^2(Z\alpha)^4$	-0.0017
18	Nuclear structure correction from $2\gamma$ amplitudes of order $(Z\alpha)^5$	$0.180 \pm 0.005$
19	Nuclear structure and VP correction in $2\gamma$ interaction of order $\alpha(Z\alpha)^5$	0.0033
20	Radiative corrections in muon line with nuclear structure of order $\alpha(Z\alpha)^5$	0.0045
21	Proton polarizability correction	$0.10 \pm 0.02$
22	Recoil correction of order $(Z\alpha)^5$	-0.2879
23	Recoil correction of order $(Z\alpha)^6$	0.0013
24	Correction to muon self-energy and muon form factors	-5.0876
25	Radiative-recoil corrections of order $\alpha(Z\alpha)^5$ and proton form factor correction $Z^2\alpha(Z\alpha)^4$	-0.0724
26	Nuclear structure correction of order $(Z\alpha)^6$	-0.0088
27	Contribution of muon form factors $F_1'(0), F_2(0)$	-0.0112
28	VP correction with muon self-energy	-0.0294
29	Hadronic vacuum polarization correction	0.0830
30	Contribution of one-meson exchange	-0.1059
31	Radiative corrections of order $\alpha(Z\alpha)^6$	0.0021
32	Summary contribution	2 249 398.5478

(2S-4P) transition in hydrogen was measured:  $\Delta\nu_{2S-4P} = 616\,520\,931\,626.8(2.3)$  kHz, and the extracted value  $r_p = 0.8335(95)$  fm turned out to be in agreement with the CREMA results [9].

To investigate the puzzle of the proton radius, the PRad experiment was proposed in 2011 (JLAB E12-11-1062) and was successfully carried out in 2016 at the Thomas Jeffer-

son National Accelerator Facility with electron beams with energies of 1.1 and 2.2 GeV. In the experiment, the elastic scattering cross sections ( $e-p$ ) were measured at unprecedentedly low values of the square of the momentum transfer with an accuracy of 1%. The value of the charge radius of the proton was  $r_p = 0.831 \pm 0.007(stat) \pm 0.012(syst)$  fm [12], which is less than the average value of  $r_p$  from previous

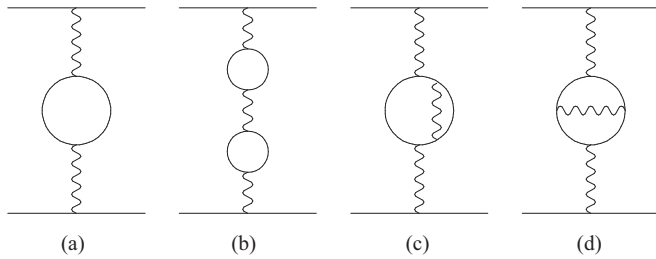


FIG. 1. Effects of one- and two-loop vacuum polarization in one-photon interaction.

experiments on elastic scattering ( $e-p$ ) but is consistent with spectroscopic results for the muonic hydrogen atom within experimental uncertainties.

A new measurement of the Lamb shift in hydrogen ( $n = 2$ ) was reported in Ref. [13]:  $\Delta E^{L_s} = 1057.8298(32)$  MHz [909.8717(32) MHz]. The value of the proton charge radius, which was obtained from this experiment,  $r_p = 0.833(10)$  fm, agrees with the spectroscopic data for muonic atoms.

To solve the problem of the proton charge radius, the MUSE collaboration is planning an experiment to simultaneously measure the cross sections for scattering of electrons and muons by protons [14]. This experiment will make it possible to determine the charge radii of the proton independently in two reactions and test lepton universality with an accuracy of an order of magnitude superior to previous scattering experiments.

It should be noted that in the recent experiment [15], a new measurement of the frequency of the two-photon transition ( $1S-3S$ ) in hydrogen was carried out with a relative error  $9 \times 10^{-13}$ :  $\Delta \nu_{1S-3S}^{2017} = 2922\,743\,278\,671.0(4.9)$  kHz. The value of the charge radius extracted from this experimental result,  $r_p = 0.877(13)$  fm, is in good agreement with the value recommended by the CODATA [16].

The experimental accuracy of measuring the energy intervals between the  $S$  levels of the hydrogen atom is very high [17]. The frequency interval between  $1S$  and  $2S$  states was measured in muonium [18] in good agreement with the QED prediction [19]. A new experiment with muonium MUMASS (muonium laser spectroscopy) [20] is aiming for a 1000-fold improvement in the determination of the  $1S-2S$  transition frequency (with accuracy 10 kHz or 4 ppt). An analogous experiment for the helium ion is now at the final

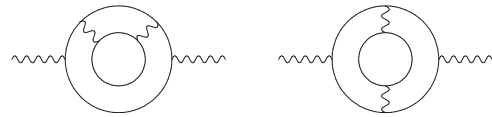


FIG. 3. Effects of three-loop vacuum polarization with two fermionic cycles in one-photon interaction.

stage [21]. There is a clear prospect of using such intervals to search for the effects of New Physics beyond the Standard Model. Spectroscopy of purely lepton systems, as well as light muonic atoms, can help in assessing the possible manifestations of spin-dependent and spin-independent forces of dark matter. The result of the experiment [15] in electron hydrogen posed, in our opinion, two problems. First, it is necessary to reanalyze the theoretical calculation of the various contributions to the ( $3S-1S$ ) interval in hydrogen in order to obtain the total theoretical value for the ( $3S-1S$ ) transition frequency and extract the proton charge radius (see the recent work [22]). The situation with the experiment [15], which gives a different magnitude for the charge radius of the proton in comparison with [11–13], requires a new consideration. The discrepancy in the proton charge radii of 0.03 fm can be due to contributions of order 100 kHz. Second, it is useful to have a precise theoretical calculation of the ( $3S-1S$ ) energy interval in muonic hydrogen as a guideline for possible future experiments with muonic hydrogen. This work is aimed at solving the second problem.

The investigations with muonic hydrogen atoms in Refs. [23,24] show that two quenching channels affect the long-lived  $\mu p(2S)$  atoms. During a collision with a  $H_2$  molecule, the  $2S$  state can be mixed with the  $2P$  state allowing an electric dipole transition to the ground state with emission of a  $K_\alpha$  photon:  $\mu p(2S) + H_2 \rightarrow \mu p(\alpha|2S + \beta|2P \rangle) + H_2 \rightarrow \mu p(1S) + H_2 + K_\alpha$ . The second quenching channel relevant for the  $\mu p(2S)$  atoms is a nonradiative de-excitation mechanism to the  $1S$  ground state: during the resonant formation of an excited muonic molecule followed by its autodissociation  $\mu p(2S) + H \rightarrow \mu p(1S) +$  and, the ( $2S-1S$ ) transition energy (1.9 keV) is distributed among the  $\mu p$  atom and the proton as kinetic energy. Similar studies of the ( $3S \rightarrow 2P$ ) transitions would make it possible to determine the frequency of the ( $3S-1S$ ) transition. In this work, we assume that experimental measurement of the transition frequency ( $3S-1S$ ) is possible.

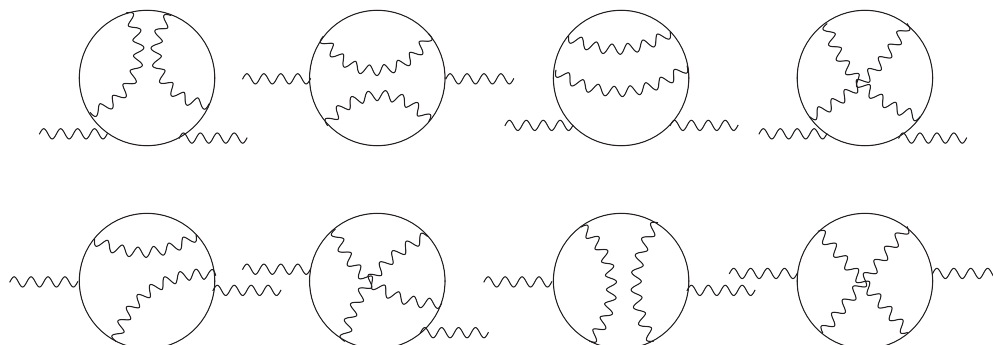


FIG. 2. Effects of three-loop vacuum polarization with one fermionic cycle in one-photon interaction.

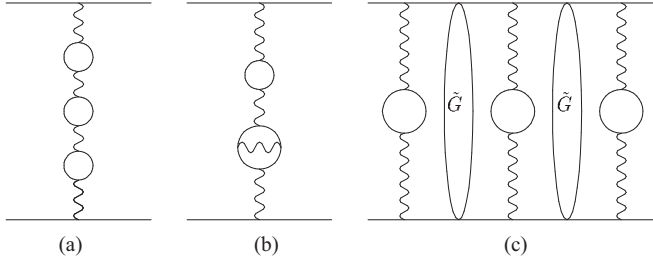


FIG. 4. Effects of three-loop vacuum polarization in one-photon interaction and third-order perturbation theory.

## II. EFFECTS OF VACUUM POLARIZATION IN ONE-PHOTON INTERACTION

The main parameters of nuclei, such as the charge radius, quadrupole moment, magnetic octupole moment, etc., are known primarily from experiments on scattering of leptons on nuclei, which have been carried out for many years. The accuracy of their determination is not very high. Another approach to the study of these parameters is related to the measurement of various spectroscopic intervals in electronic or muonic atoms and ions with such nuclei. We consider one of such basic intervals ( $3S-1S$ ), which is measured for the electron hydrogen atom with very high accuracy. One of the leading contributions to this energy interval is determined by the proton charge radius, and, therefore, the charge radius can be extracted from the corresponding experimental data. For this to be possible, it is necessary to perform a theoretical calculation of the interval ( $3S-1S$ ) with high accuracy.

Our approach to the precision calculation of the energy range ( $3S-1S$ ) is based on the quasipotential method in quantum electrodynamics [25–27]. The two-particle bound state is described by the Schrödinger equation, and the main contribution to the particle interaction operator is determined by the Breit Hamiltonian. A number of important results in the study of the energy levels of muonic atoms have been obtained in

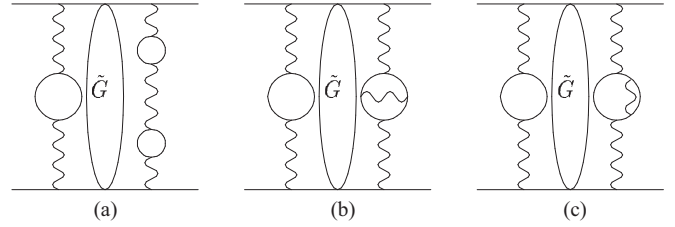


FIG. 6. Three-loop vacuum polarization corrections in the second-order PT.  $\tilde{G}$  is the reduced Coulomb Green's function.

Refs. [28–30] (see Ref. [19] for other references). The main contribution to the fine structure of the  $S$ -wave spectrum of hydrogen-like atoms consisting of particles with masses  $m_1$  (the muon mass)  $m_2$  (the proton mass) can be represented with an accuracy of  $O((Z\alpha)^6)$  ( $\mu$  is the reduced mass) in the following form [19]:

$$E_n = m_1 + m_2 - \frac{\mu(Z\alpha)^2}{2n^2} - \frac{\mu(Z\alpha)^4}{2n^3} \left( 1 - \frac{3}{4n} + \frac{\mu^2}{4m_1 m_2 n} \right) - \frac{m_1(Z\alpha)^6}{16n^6} (2n^3 + 6n^2 - 12n + 5). \quad (1)$$

This formula correctly takes into account the recoil correction  $m_1^2/m_2^2(Z\alpha)^4$  for nuclei with spin 1/2 [19] (see Sec. IV). Recoil effects of order  $(Z\alpha)^6$  are not taken into account in formula (1) and are discussed in Sec. V.

To extract the charge radius of a proton with high accuracy from the measurement of some spectroscopic interval, it is necessary to calculate corrections of a high order of smallness in terms of the fine structure constant and the particle mass ratio. Numerical values of the same effects presented in the Feynman diagrams differ significantly in the case of electronic and muonic hydrogen. In what follows, we consider the calculation of contributions to the ( $3S-1S$ ) interval in order of importance for muonic hydrogen. Numerical values of contributions are shown in separate lines of Table I. In the second

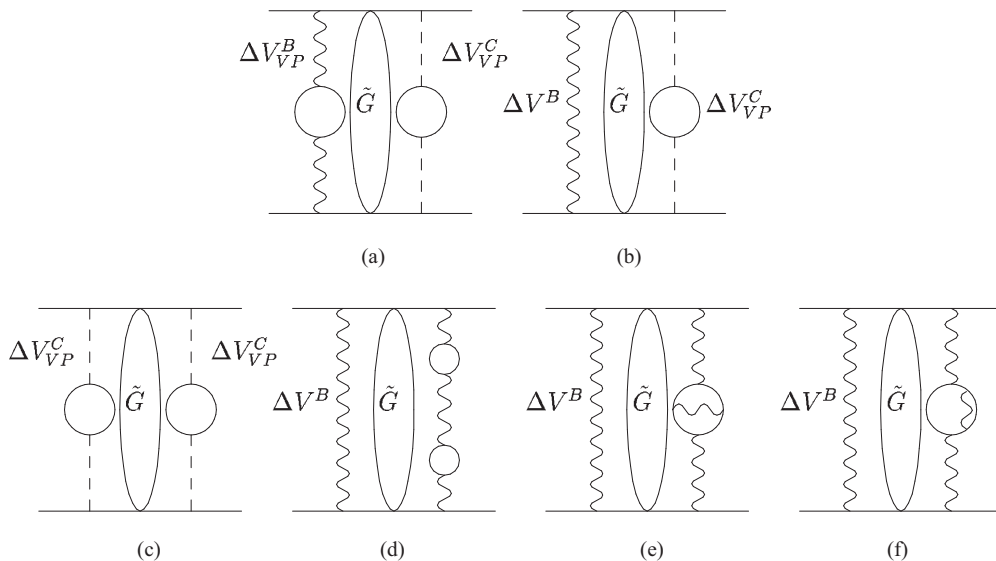


FIG. 5. Effects of one- and two-loop vacuum polarization in second-order perturbation theory.  $\tilde{G}$  is the reduced Coulomb Green's function. The dashed line represents the Coulomb photon. The wavy line denotes the Breit potential (relativistic correction).

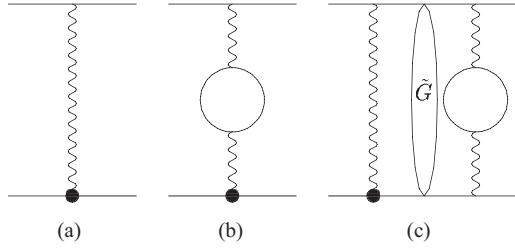


FIG. 7. Corrections to the nuclear structure and the polarization of vacuum in the first-order PT (FOPT) and the second-order PT (SOPT).

column of Table I we indicate the order of the considered contribution for muonic hydrogen.

An important class of corrections to energy levels are corrections for the vacuum polarization (VP). Although their value decreases with an increase in the number of loops in the polarization operator, it is necessary to take into account contributions up to three loops inclusively to achieve a high calculation accuracy. The one-loop vacuum polarization leads to a modification of the Coulomb potential and is determined

in the coordinate representation by the following expression (the subscript  $vp$  denotes here and below the electronic polarization of the vacuum, and the superscript  $C$  the contribution of the Coulomb interaction):

$$V_{vp}^C(r) = \frac{\alpha}{3\pi} \int_1^\infty d\xi \rho(\xi) \left( -\frac{Z\alpha}{r} e^{-2m_e \xi r} \right),$$

$$\rho(\xi) = \frac{\sqrt{\xi^2 - 1}(2\xi^2 + 1)}{\xi^4}. \quad (2)$$

In the first-order perturbation theory (PT), it is necessary to calculate the matrix elements of the operator (2) from the wave functions of 1S and 3S states, which have the following form:

$$\psi_{100}(r) = \frac{W^{3/2}}{\sqrt{\pi}} e^{-Wr}, \quad W = \mu Z \alpha,$$

$$\psi_{300}(r) = \frac{W^{3/2}}{3\sqrt{3}\pi} e^{-Wr/3} \left[ 1 - \frac{2}{3}Wr + \frac{2}{27}(Wr)^2 \right]. \quad (3)$$

Analytical calculation of matrix elements gives the following shifts of energy levels 1S and 3S ( $b_1 = m_e/W$ ,  $W = \mu Z \alpha$ ,  $Z = 1$  is the charge of the proton):

$$\Delta E_{vp}(1S) = -\frac{4\mu(Z\alpha)^2 \alpha \sqrt{b_1^2 - 1} (12\pi b_1^3 - 24b_1^2 + 9\pi b_1 - 22) - 6(4b_1^4 + b_1^2 - 2) \sec^{-1}(b_1)}{3\pi \cdot 6\sqrt{b_1^2 - 1}}, \quad (4)$$

$$\Delta E_{vp}(3S) = -\frac{4\mu\alpha(Z\alpha)^2}{81\pi} \frac{1}{16(9b_1^2 - 1)^{9/2}} \left\{ \sqrt{9b_1^2 - 1} [9b_1 [-7243344b_1^9 + 3006396b_1^7 - 447768b_1^5 + 27999b_1^3 + 18\pi(1 - 9b_1^2)^4(92b_1^2 + 1) - 224b_1] - 64] - 3i[81b_1^2(27\{[108b_1^2(828b_1^4 - 405b_1^2 + 76) - 703]b_1^2 + 26\}b_1^2 + 4) - 8] \ln \left( \frac{3ib_1}{\sqrt{9b_1^2 - 1} - i} \right) \right\}. \quad (5)$$

It is useful to note that the  $1/b_1 = \mu Z \alpha / m_e = 1.356$ , so the parameter  $1/b_1$  cannot be used as an expansion parameter, since it is not small. The corresponding numerical value of these contributions for the (3S-1S) interval is presented in Table I (line 2). It is written for definiteness with an accuracy of up to four digits after the decimal point, since the errors connected with errors in the determination of fundamental physical constants are significantly less. The expressions (4) and (5) can also be used to numerically estimate the contribution of muon vacuum polarization in muonic hydrogen, replacing the electron mass with the muon mass. In this case, numerical value of the contribution decreases sharply, which is connected with an increase in general order of such contribution due to the factor  $\alpha^2$  (see line 3 in Table I). Numerical value of this correction is somewhat different from that which is obtained using an analytical expression in leading order  $\Delta E_{mvp}(3S-1S) = 104\alpha(Z\alpha)^4 \mu^3 / 405\pi m_1^2 = 0.1298$  meV. It appears in (4) and (5) due to corrections of higher order and must be taken into account if we want to use this interval for more accurate obtaining of the proton charge radius. The operator (2) also makes contributions in higher orders of perturbation theory, which are considered below. In one-photon interaction there are also contributions of two- and three-loop vacuum polarization (see Figs. 1–4).

In the case of contributions from the fourth-order polarization operator (Fig. 1), one can construct the interaction potential of particles and the shift of energy levels in integral form using the replacement in the photon propagator in the momentum representation [31]:

$$\frac{1}{k^2} \rightarrow \frac{2}{3} \left( \frac{\alpha}{\pi} \right)^2 \int_0^1 \frac{f(v) dv}{4m_e^2 + k^2(1-v^2)},$$

$$f(v) = v \left\{ (3-v^2)(1+v^2) \left[ Li_2 \left( -\frac{1-v}{1+v} \right) + 2Li_2 \left( \frac{1-v}{1+v} \right) + \frac{3}{2} \ln \frac{1+v}{1-v} \ln \frac{1+v}{2} - \ln \frac{1+v}{1-v} \ln v \right] \right.$$

$$\left. + \left[ \frac{11}{16}(3-v^2)(1+v^2) + \frac{v^4}{4} \right] \ln \frac{1+v}{1-v} + \left[ \frac{3}{2}v(3-v^2) \ln \frac{1-v^2}{4} - 2v(3-v^2) \ln v \right] + \frac{3}{8}v(5-3v^2) \right\}, \quad (6)$$



where  $Li_2(z)$  is the Euler dilogarithm. Then, in the coordinate representation, the particle interaction operator takes the form convenient for the subsequent calculation of the energy shift:

$$\Delta V_{1\gamma, 2-loop\ v\rho}^C(r) = -\frac{2Z\alpha}{3r} \left(\frac{\alpha}{\pi}\right)^2 \int_0^1 \frac{f(v) dv}{1-v^2} e^{-\frac{2m_e r}{\sqrt{1-v^2}}}. \quad (7)$$

The numerical contribution (7) is included in Table I together with another contribution of the two-loop vacuum polarization with two successive loops, which is denoted below by the subscript  $v\rho$ - $v\rho$ . In the momentum representation, the corresponding particle interaction potential has the form

$$\begin{aligned} V_{v\rho-v\rho}^C(k^2) &= -4\pi(Z\alpha) \frac{\alpha^2}{9\pi^2} \int_1^\infty \rho(\xi) d\xi \int_1^\infty \rho(\eta) d\eta \frac{k^2}{(k^2 + 4m_e^2 \xi^2)(k^2 + 4m_e^2 \eta^2)} \\ &= -\frac{2\alpha^2(Z\alpha)}{9\pi} \int_1^\infty \rho(\xi) d\xi \int_1^\infty \rho(\eta) d\eta \left[ \frac{1}{k^2 + 4m_e^2 \xi^2} + \frac{1}{k^2 + 4m_e^2 \eta^2} - \frac{(\xi^2 + \eta^2)}{(\eta^2 - \xi^2)} \left( \frac{1}{k^2 + 4m_e^2 \xi^2} - \frac{1}{k^2 + 4m_e^2 \eta^2} \right) \right]. \end{aligned} \quad (8)$$

After the Fourier transform, (8) takes the form of a superposition of the Yukawa potentials, distributed with a certain density:

$$V_{1\gamma, v\rho-v\rho}^C(r) = \frac{\alpha^2}{9\pi^2} \int_1^\infty \rho(\xi) d\xi \int_1^\infty \rho(\eta) d\eta \left(-\frac{Z\alpha}{r}\right) \frac{1}{(\xi^2 - \eta^2)} (\xi^2 e^{-2m_e \xi r} - \eta^2 e^{-2m_e \eta r}). \quad (9)$$

When calculating the matrix elements (7) and (9), the integration over the particle coordinates is performed analytically, and the subsequent integration over the spectral parameters is numerical. The contributions (7) and (9) are of order  $\alpha^2(Z\alpha)^2$  for muonic hydrogen and are numerically large (see line 6 in the table), so it is necessary to consider corrections of the next order in  $\alpha$ . In the case of muon vacuum polarization, the two-loop contributions (7) and (9) are equal to 0.0011 meV have the order  $\alpha^2(Z\alpha)^4$  and are determined by the well-known analytical formula (see Sec. IV [19]). We have included it also in the full result in line 6.

Turning to the contributions of the sixth-order polarization operator (in this case, the number 6 means the number of interaction vertices in the vacuum loop), we note that they were studied in the case of the Lamb shift ( $2P$ - $2S$ ) in Refs. [32,33]. It is convenient to divide this contribution into two parts with one ( $1f$ ) and two ( $2f$ ) fermionic cycles. It is useful to note that in Ref. [34] a general parametric formula was obtained for the contributions in Figs. 2 and 3, but it is difficult to use it to obtain numerical estimates due to the remaining multiple integrals over the Feynman and spectral parameters, as well as the renormalization procedure. A more convenient formula for practical use was obtained in Refs. [32,35] for the contribution of eight diagrams:

$$\begin{aligned} \Pi_3^{(1)}(z) &= \tilde{\Pi}_3^{(1)}(z) - 4\Pi_2(z) - (1-z)G(z) \left( \frac{9}{4}G(z) + \frac{31}{16} + \frac{229}{32z} + \frac{229}{32z} + \frac{173}{96} \right), \\ \tilde{\Pi}_3^{(1)}(z) &= \tilde{\Pi}_3^{(1)}(z)(-\infty) + \frac{(1+\omega)^2}{(1-\omega)} \frac{(\tilde{a}_0 + \tilde{a}_1\omega + \tilde{a}_2\omega + \tilde{a}_3\omega)}{(\tilde{b}_0 + \tilde{b}_1\omega + \tilde{b}_2\omega + \tilde{b}_3\omega)}, \end{aligned} \quad (10)$$

and the explicit form of the functions involved and their asymptotic values can be found in Refs. [32,35]. The Padé approximation coefficients  $\tilde{a}_i$ ,  $\tilde{b}_i$  are written out in Ref. [33]. The general formula for the contribution of the polarization operator (10) (the contribution of eight diagrams in Fig. 2) to the shift ( $3S$ - $1S$ ) has the following form:

$$\begin{aligned} \Delta E_{1\gamma}^{1f}(3S-1S) &= \frac{64}{\pi} \left(\frac{\alpha}{\pi}\right)^3 \mu(Z\alpha)^2 \int_0^\infty \frac{s^2 \rho_1(s)}{(4+9s^2)^6(4+s^2)^2} \Pi_3^{(1)}\left(\frac{s^2}{4b_1^2}\right), \\ \rho_1(s) &= (69\,632 + s^2\{-71\,936 + 3s^2[239\,360 + 81s^2(3296 + 2688s^2 + 1053s^4)]\}), \end{aligned} \quad (11)$$

and the numerical value of the contribution to the ( $3S$ - $1S$ ) interval in muonic hydrogen is

$$\Delta E_{1\gamma}^{1f}(3S-1S) = 0.0169 \text{ meV}. \quad (12)$$

The diagrams with two fermionic cycles in Fig. 3 can be considered as corrections to the mass and vertex operators. In this case, the dispersion relation can be used for the second-order polarization operator. The effective propagator of a virtual photon in these diagrams can be represented as

$$\frac{-i}{k^2 + i0} \left( g_{\mu\lambda} - \xi \frac{k_\mu k_\lambda}{k^2} \right) \Pi_{\lambda\sigma}(k^2) \frac{-i}{k^2 + i0} \left( g_{\nu\sigma} - \xi \frac{k_\nu k_\sigma}{k^2} \right), \quad (13)$$

which, taking into account the transverse character of the polarization operator  $\Pi_{\lambda\sigma}(k^2)$ , means that the result is gauge invariant. Taking into account such contributions is important for achieving high accuracy in calculating the anomalous magnetic moment of the lepton [36,37]. The imaginary part of the polarization operator in Fig. 3 was initially represented in the form of a two-dimensional spectral integral [38], and then in an analytical form in Ref. [39], and the final formula is rather cumbersome. In

our calculations, we use the last representation of the polarization operator from Ref. [39], and the calculation formula for the contribution is

$$\Delta E_{1\gamma}^{2f}(3S-1S) = -\frac{64}{\pi} \left(\frac{\alpha}{\pi}\right)^3 \mu(Z\alpha)^2 \int_0^\infty \frac{s^2 \rho_1(s) ds}{(4+s^2)^2(4+9s^2)^6} \int_1^\infty \frac{\rho_{2f}(t,s) dt}{t(t+\frac{s^2}{4\beta^2})}, \quad (14)$$

where two-fermion spectral density  $\rho_{2f}(s,t)$  is taken from Ref. [39], and the numerical value (14) for muonic hydrogen ( $-0.0158$  meV) differs in sign from (11). The sum of corrections (11) and (14) is equal to  $0.0246$  meV.

The remaining three-loop contributions in Fig. 3 with successive loops can be calculated in the same way as the two-loop ones in Fig. 1, by constructing the interaction potentials as was done in (8) and (9). General expressions for these potentials in the coordinate representation are the following [25,40]:

$$V_{vp-vp-vp}^C(r) = -\frac{Z\alpha}{r} \frac{\alpha^3}{(3\pi)^3} \int_1^\infty \rho(\xi) d\xi \int_1^\infty \rho(\eta) d\eta \int_1^\infty \rho(\zeta) d\zeta \times \left[ e^{-2m_e \zeta r} \frac{\zeta^4}{(\xi^2 - \zeta^2)(\eta^2 - \zeta^2)} + e^{-2m_e \xi r} \frac{\xi^4}{(\zeta^2 - \xi^2)(\eta^2 - \xi^2)} + e^{-2m_e \eta r} \frac{\eta^4}{(\xi^2 - \eta^2)(\zeta^2 - \eta^2)} \right], \quad (15)$$

$$V_{vp2-loop vp}^C = -\frac{4\mu\alpha^3(Z\alpha)}{9\pi^3 r} \int_1^\infty \rho(\xi) d\xi \int_1^\infty \frac{f(\eta) d\eta}{\eta} \left[ e^{-2m_e \eta r} \frac{\eta^2}{\eta^2 - \xi^2} - e^{-2m_e \xi r} \frac{\xi^2}{\eta^2 - \xi^2} \right]. \quad (16)$$

The corrections in the energy spectrum corresponding to these interactions are presented in integral form over three spectral parameters and calculated numerically. The total numerical value of the three-loop contribution of the vacuum polarization from the  $1\gamma$ -interaction is presented in Table I in a separate line 7. In the case of muon vacuum polarization, the contribution of the third-order polarization operator obtained by formula (58) [19] is negligible small.

### III. EFFECTS OF VACUUM POLARIZATION AND RELATIVISTIC CORRECTIONS

The Breit potential contributes to the energy of  $S$ -states in the leading order  $(Z\alpha)^4$ . The effect of vacuum polarization leads to a change not only in the Coulomb potential, but also in other terms in the Breit potential, which will contribute to the energy spectrum of order  $\alpha(Z\alpha)^4$ . This order of contribution suggests that the numerical values of the corrections can be significant. The modification of the Breit potential due to the one-loop vacuum polarization is determined in the case of  $S$ -states by the following terms (the superscript  $B$  denotes the Breit potential) [30,40,41]:

$$\Delta V_{vp}^B(r) = \frac{\alpha}{3\pi} \int_1^\infty \rho(\xi) d\xi \sum_{i=1}^3 \Delta V_{i,vp}^B(r), \quad (17)$$

$$\Delta V_{1,vp}^B = \frac{Z\alpha}{8} \left( \frac{1}{m_1^2} + \frac{1}{m_2^2} \right) \left[ 4\pi \delta(\mathbf{r}) - \frac{4m_e^2 \xi^2}{r} e^{-2m_e \xi r} \right], \quad (18)$$

$$\Delta V_{2,vp}^B = -\frac{Z\alpha m_e^2 \xi^2}{m_1 m_2 r} e^{-2m_e \xi r} (1 - m_e \xi r), \quad (19)$$

$$\Delta V_{3,vp}^B = -\frac{Z\alpha}{2m_1 m_2} p_i \frac{e^{-2m_e \xi r}}{r} \left[ \delta_{ij} + \frac{r_i r_j}{r^2} (1 + 2m_e \xi r) \right] p_j. \quad (20)$$

The largest numerical contribution (more than 80%) comes from the term  $\Delta V_{1,vp}^B$ , whose matrix elements are calculated analytically for  $1S$  and  $3S$  states:

$$\Delta E_{1,vp}^B(1S) = \frac{\alpha(Z\alpha)^4 \mu^3}{18\pi} \left( \frac{1}{m_1^2} + \frac{1}{m_2^2} \right) \left[ (1 + 6b_1^2 - 3b_1^3 \pi) + \frac{1}{\sqrt{1-b_1^2}} (6 - 3b_1^2 + 6b_1^4) \ln \frac{1 + \sqrt{1-b_1^2}}{b_1} \right], \quad (21)$$

$$\Delta E_{1,vp}^B(3S) = \frac{\alpha(Z\alpha)^4 \mu^3}{1944\pi (1-9b_1^2)^4} \left( \frac{1}{m_1^2} + \frac{1}{m_2^2} \right) \left( 9(9b_1 \{ 3b_1 [6(972b_1^4 - 414b_1^2 - 5)b_1^2 + 19] - 4\pi(1-9b_1^2)^4 \} - 116)b_1^2 + 32 + \frac{1}{(1-9b_1^2)^{1/2}} \left\{ 3[81(9b_1^2 \{ [162b_1^2(36b_1^4 - 18b_1^2 + 5) - 89]b_1^2 + 10\} - 4)b_1^2 + 8] \ln \left( \frac{3b_1 \sqrt{1-9b_1^2}}{-1+9b_1^2 + \sqrt{1-9b_1^2}} \right) \right\} \right). \quad (22)$$

The total contribution of relativistic corrections taking into account the one-loop vacuum polarization is presented in line 8 of Table I. In order to increase the accuracy of the calculation we also take into account the contribution of relativistic corrections with effects of two-loop vacuum polarization of order  $\alpha^2(Z\alpha)^4$ . The main term in the interaction potential is

$$\Delta V_{1,2loop-vp}^B = \frac{\alpha^2(Z\alpha)}{12\pi^2} \left( \frac{1}{m_1^2} + \frac{1}{m_2^2} \right) \int_0^1 \frac{f(v) dv}{1-v^2} \left[ 4\pi\delta(\mathbf{r}) - \frac{4m_e^2}{r(1-v^2)} e^{-\frac{2m_e r}{\sqrt{1-v^2}}} \right], \quad (23)$$

and the calculation of matrix elements is carried out similarly to (21) and (22).

In the second order of perturbation theory, there are a number of contributions in which the potentials  $\Delta V_{vp}^C$ ,  $\Delta V^B$  (Breit potential),  $\Delta V_{vp}^B$  are considered as perturbation operators (the subscript *sopt* denotes the second-order PT contribution):

$$\begin{aligned} \Delta E_{sopt}^{B,vp} &= \langle \psi | \Delta V_{vp}^C \tilde{G} \Delta V_{vp}^C | \psi \rangle + 2 \langle \psi | \Delta V^B \tilde{G} \Delta V_{vp}^C | \psi \rangle \\ &+ 2 \langle \psi | \Delta V_{vp}^B \tilde{G} \Delta V_{vp}^C | \psi \rangle + 2 \langle \psi | \Delta V^B \tilde{G} \Delta V_{vp,vp}^C | \psi \rangle, \end{aligned} \quad (24)$$

$$\Delta V^B = -\frac{\mathbf{p}^4}{8m_1^3} - \frac{\mathbf{p}^4}{8m_2^3} + \frac{\pi Z\alpha}{2} \left( \frac{1}{m_1^2} + \frac{1}{m_2^2} \right) \delta(\mathbf{r}) - \frac{Z\alpha}{2m_1 m_2 r} \left[ \mathbf{p}^2 + \frac{\mathbf{r}(\mathbf{r}\mathbf{p})\mathbf{p}}{r^2} \right]. \quad (25)$$

Such contributions, presented for a clarity in the diagrams in Fig. 5, can be considered as one- and two-loop vacuum polarization corrections with account for relativistic effects. The reduced Coulomb Green's function of 1S and 2S states has the well-known form [42]. To derive the Green's function for the 3S state, we used the general expression for the Coulomb Green's function [43,44] in terms of the product of Whittaker's functions. After subtracting the pole term, the following expression is obtained for the reduced Green's function of the 3S state:

$$\begin{aligned} G_{3S}(\mathbf{r}_1, \mathbf{r}_2) &= -\frac{Z\alpha\mu^2}{13\,122\pi r_1 r_2} e^{-\frac{1}{3}(x_1+x_2)} g_{3S}(x_1, x_2), \\ g_{3S}(x_1, x_2) &= 18x_{<}[2(x_{<} - 9)x_{<} + 27][2(x_{>} - 9)x_{>} + 27]x_{>} \left[ \text{Ei}\left(\frac{2x_{<}}{3}\right) - \ln(x_{<}) - \ln\left(\frac{4x_{>}}{9}\right) \right] \\ &- 4x_{<}[2(x_{<} - 9)x_{<} + 27]x_{>}^4 + 2(-27e^{\frac{2}{3}x_{<}}[x_{<}(2x_{<} - 15) + 9] + x_{<}\{-36\gamma[2(x_{<} - 9)x_{<} + 27] \\ &- 2x_{<}[x_{<}(2x_{<} - 135) + 891] + 1701\} + 243)x_{>}^3 + 18(27e^{\frac{2}{3}x_{<}}[x_{<}(2x_{<} - 15) + 9] \\ &+ x_{<}\{36\gamma[2(x_{<} - 9)x_{<} + 27] + 2x_{<}[x_{<}(2x_{<} - 99) + 567] - 729\} - 243)x_{>}^2 \\ &+ 27(-27e^{\frac{2}{3}x_{<}}[x_{<}(2x_{<} - 15) + 9] + x_{<}\{-2(x_{<} - 27)x_{<}(2x_{<} - 9) - 36\gamma[2(x_{<} - 9)x_{<} \\ &+ 27] - 243\} + 243)x_{>} + 243x_{<}[2(x_{<} - 9)x_{<} + 27], \end{aligned} \quad (26)$$

where  $x_{<} = \min(x_1, x_2)$ ,  $x_{>} = \max(x_1, x_2)$ ,  $x_i = W r_i$ ,  $\gamma$  is the Euler constant.

When calculating corrections in the second-order PT, it is also necessary to know the reduced Coulomb Green's function with one zero argument, which is obtained from (26) by expanding at  $r_2 = 0$  in the form

$$G_{3S}(\mathbf{r}) = \frac{Z\alpha\mu^2}{3\pi x} e^{-\frac{1}{3}x} \left[ 4x^4 - 144x^3 + 648x^2 + 18\gamma(2x^2 - 18x + 27)x + 18(2x^2 - 18x + 27)x \ln\left(\frac{2x}{3}\right) - 243 \right], \quad (27)$$

where the dimensionless variable  $x = W r$ .

Among the amplitudes in Fig. 5, the largest contribution of order  $\alpha^2(Z\alpha)^2$  is given by the amplitude (c), which contains two Coulomb potentials corrected for the vacuum polarization. An integration over coordinates can also be carried out analytically and over spectral parameters numerically. Since, after the integration over coordinates, the result has a cumbersome form, we present here the initial integral expression for this correction and its numerical value in the shift (3S-1S):

$$\Delta E_{sopt}^{vp,vp}(1S) = -\frac{16\mu\alpha^2(Z\alpha)^2}{9\pi^2} \int_1^\infty \rho(\xi) d\xi \int_1^\infty \rho(\eta) d\eta \int_0^\infty x_1 e^{-x_1(1-\frac{2m_e\xi}{W})} dx_1 \int_0^\infty x_2 e^{-x_2(1-\frac{2m_e\eta}{W})} g_{1S}(x_1, x_2) dx_2, \quad (28)$$

$$\begin{aligned} \Delta E_{sopt}^{vp,vp}(3S) &= -\frac{8\mu\alpha^2(Z\alpha)^2}{1\,594\,323\pi^2} \int_1^\infty \rho(\xi) d\xi \int_1^\infty \rho(\eta) d\eta \\ &\times \int_0^\infty \left( 1 - \frac{2x_1}{3} + \frac{2x_1^2}{27} \right) e^{-x_1(2/3-\frac{2m_e\xi}{W})} dx_1 \int_0^\infty \left( 1 - \frac{2x_2}{3} + \frac{2x_2^2}{27} \right) e^{-x_2(2/3-\frac{2m_e\eta}{W})} g_{3S}(x_1, x_2) dx_2, \end{aligned} \quad (29)$$

$$\Delta E_{sopt}^{vp,vp}(3S - 1S) = 1.9955 \text{ meV}. \quad (30)$$



When calculating other corrections in the second-order PT with the Breit potential, transformations of the original matrix elements are used to bring them to a form convenient for the integration. So, for example, when calculating the contribution of the amplitude in Fig. 5(b), the following matrix element ( $n$  is the principal quantum number) appears:

$$\begin{aligned} M_{nS} &= \langle \psi_{nS} | \frac{\mathbf{p}^4}{(2\mu)^2} \sum'_m \frac{|\psi_m\rangle\langle\psi_m|}{E_n - E_m} \Delta V_{vp}^C | \psi_{nS} \rangle = \langle \psi_{nS} | \left( E_n + \frac{Z\alpha}{r} \right) \left( \hat{H}_0 + \frac{Z\alpha}{r} \right) \\ &\quad \times \sum'_m \frac{|\psi_m\rangle\langle\psi_m|}{E_n - E_m} \Delta V_{vp}^C | \psi_{nS} \rangle = \langle \psi_{nS} | \left( E_n + \frac{Z\alpha}{r} \right)^2 \tilde{G} \Delta V_{vp}^C | \psi_{nS} \rangle \\ &\quad - \langle \psi_{nS} | \frac{Z\alpha}{r} \Delta V_{vp}^C | \psi_{nS} \rangle + \langle \psi_{nS} | \frac{Z\alpha}{r} | \psi_{nS} \rangle \langle \psi_{nS} | \Delta V_{vp}^C | \psi_{nS} \rangle. \end{aligned} \quad (31)$$

After integration over coordinates we obtain an integral expressions of the following form:

$$\begin{aligned} M_{1S} &= \frac{\mu^2 \alpha (Z\alpha)^4}{12\pi} \int_1^\infty \frac{\rho(s) ds}{(b_1 s + 1)^3} [13 + 25b_1 s + 8b_1^2 s^2 + 8(1 + b_1 s) \ln(1 + b_1 s)], \\ M_{3S} &= \frac{\mu^2 \alpha (Z\alpha)^4}{972\pi} \int_1^\infty \frac{\rho(s) ds}{(3b_1 s + 1)^7} [52 488 b_1^6 s^6 + 50 301 b_1^5 s^5 + 23 571 b_1^4 s^4 + 21 546 b_1^3 s^3 \\ &\quad + 1998 b_1^2 s^2 + 72(729 b_1^5 s^5 + 243 b_1^4 s^4 + 162 b_1^3 s^3 + 54 b_1^2 s^2 + 3b_1 s + 1) \ln(3b_1 s + 1) + 651 b_1 s + 37]. \end{aligned} \quad (32)$$

Another term in the Breit potential, proportional to  $\delta(\mathbf{r})$ , gives the Green's function with one zero argument  $\tilde{G}_{nS}(\mathbf{r}, 0)$  when calculating the matrix elements. The structure of the resulting expression after coordinate integration is quite similar to (32) and (33):

$$\begin{aligned} \Delta E_2^{B,vp}(1S) &= \frac{\mu^3 \alpha (Z\alpha)^4}{6\pi} \left( \frac{1}{m_1^2} + \frac{1}{m_2^2} \right) \int_1^\infty \frac{\rho(s) ds}{(1 + b_1 s)^3} [2b_1^2 s^2 + 7b_1 s + 2(b_1 s + 1) \ln(b_1 s + 1) + 3], \\ \Delta E_2^{B,vp}(3S) &= \frac{\mu^2 \alpha (Z\alpha)^4}{3\pi} \left( \frac{1}{m_1^2} + \frac{1}{m_2^2} \right) \int_1^\infty \frac{\rho(s) ds}{(1 + 2b_1 s)^7} \{ -2(3b_1 s + 1)(243b_1^4 s^4 + 54b_1^2 s^2 + 1) \\ &\quad \times \ln(3b_1 s + 1) - 3b_1 s [6b_1 s (b_1 s \{ 3b_1 s [9b_1 s (3b_1 s + 2) + 4] + 28\} + 1) + 5] - 1 \}. \end{aligned} \quad (34)$$

Finally, the third term from (25) gives, in the second order, the correction for recoil, which we represent in integral form as (32), (33), (34), and (35):

$$\begin{aligned} \Delta E_3^{B,vp}(1S) &= -\frac{\mu^3 \alpha (Z\alpha)^4}{3\pi m_1 m_2} \int_1^\infty \frac{\rho(s) ds}{(1 + b_1 s)^3} [5b_1 s + 4(b_1 s + 1) \ln(b_1 s + 1) + 3], \\ \Delta E_3^{B,vp}(3S) &= -\frac{\mu^3 \alpha (Z\alpha)^4}{3\pi m_1 m_2} \int_1^\infty \frac{\rho(s) ds}{(1 + 2b_1 s)^7} [1701 b_1^5 s^5 - 567 b_1^4 s^4 + 1998 b_1^3 s^3 + 54 b_1^2 s^2 \\ &\quad + 12(729 b_1^5 s^5 + 243 b_1^4 s^4 + 162 b_1^3 s^3 + 54 b_1^2 s^2 + 3b_1 s + 1) \ln(3b_1 s + 1) + 69 b_1 s + 5]. \end{aligned} \quad (35)$$

Numerical values of the contributions in Fig. 5 are shown in several lines: 10, 11, 12. Since the contribution of the interaction in Fig. 5(c) has the order  $\alpha^2 (Z\alpha)^2$ , then the addition of one VP loop leaves such a correction potentially important. The contribution of the three-loop VP in the second-order PT is shown in Fig. 6 (all perturbation potentials are the corrections of the vacuum polarization to the Coulomb potential). Omitting the details of the calculation of this contribution (see Ref. [26]), since they are similar to the calculation of the amplitude in Fig. 5(c), we present its numerical value in Table I (line 13).

The contribution of the three-loop vacuum polarization in the third-order PT is shown in Fig. 4(c). It is determined by the sum of two terms [45]:

$$\Delta E_{nS} = \langle \psi_{nS} | \Delta V^C \tilde{G} \Delta V^C \tilde{G} \Delta V^C | \psi_{nS} \rangle - \langle \psi_{nS} | \Delta V^C | \psi_{nS} \rangle \langle \psi_{nS} | \Delta V^C \tilde{G} \tilde{G} \Delta V^C | \psi_{nS} \rangle. \quad (36)$$

The corrections of this type are presented in the form of multiple integrals over spectral parameters as in Ref. [27] and calculated numerically (see line 14 of Table I). Numerical integration is performed with good accuracy and accepted in this work.

#### IV. CORRECTIONS TO THE NUCLEAR STRUCTURE AND VACUUM POLARIZATION

A decrease in the value of the Bohr radius of orbits in muonic atoms in comparison with electronic ones leads to the fact that the wave function of the muon overlaps strongly with the region of the proton. Expanding the charge form factor of the proton at small momentum transfers, we find that in the leading order the effect of the nuclear structure is determined in the energy range (3S-1S) by the following correction proportional to the square of the charge radius  $r_p^2$  [19] [see Fig. 7(a)] (the subscript  $str$  denotes here and below a correction for the nuclear structure; hereinafter, for the proton charge radius, we use the notation  $r_p$ ):

$$\Delta E_{str}(3S-1S) = -\frac{52\mu^3(Z\alpha)^4}{81} r_p^2 = -40.039631 r_p^2 = -28.3105 \text{ meV}, \quad (37)$$

where we have extracted the coefficient at  $r_p^2$ , and the value of the charge radius itself is taken in fm. For a numerical estimate of the contributions (39), the value of the proton charge radius from Ref. [9] is used. The next most important correction for muonic hydrogen is the correction for the structure of the nucleus of order  $(Z\alpha)^5$  of two-photon exchange amplitudes (see Fig. 8), which is expressed in terms of the Dirac  $F_1$  and Pauli  $F_2$  form factors of the proton. Neglecting the relative momenta of particles in the initial and final states, one can represent this contribution to the shift of  $S$  levels in the integral form:

$$\begin{aligned} \Delta E_{str}^{2\gamma}(3S-1S) &= \frac{26\mu^3(Z\alpha)^5}{27\pi} \delta_{l0} \int_0^\infty \frac{dk}{k} V_{2\gamma}(k), \quad V_{2\gamma}(k) = \frac{2(F_1^2 - 1)}{m_1 m_2} + \frac{8m_1[F_2(0) + 4m_2^2 F_1'(0)]}{m_2(m_1 + m_2)k} \\ &+ \frac{k^2}{2m_1^3 m_2^3} [2(F_1^2 - 1)(m_1^2 + m_2^2) + 4F_1 F_2 m_1^2 + 3F_2^2 m_1^2] + \frac{\sqrt{k^2 + 4m_1^2}}{2m_1^3 m_2(m_1^2 - m_2^2)k} \\ &\times \left\{ k^2 [2(F_1^2 - 1)m_2^2 + 4F_1 F_2 m_1^2 + 3F_2^2 m_1^2] - 8m_1^4 F_1 F_2 + \frac{16m_1^4 m_2^2 (F_1^2 - 1)}{k^2} \right\} \\ &- \frac{\sqrt{k^2 + 4m_2^2} m_1}{2m_2^3 (m_1^2 - m_2^2)k} \left\{ k^2 [2(F_1^2 - 1) + 4F_1 F_2 + 3F_2^2] - 8m_2^2 F_1 F_2 + \frac{16m_2^4 (F_1^2 - 1)}{k^2} \right\}. \end{aligned} \quad (40)$$

In numerical integration in (40), we use the parametrization of the proton form factors from [46]. Numerical result of the correction for the nuclear structure from two-photon exchange amplitudes (40) is included in Table I in line 18. The error in calculating this contribution is estimated at 1%, therefore the result is given with an accuracy of two digits after the decimal point. The magnitude of this correction in muonic hydrogen increases significantly in comparison with electron hydrogen. The contribution of two-photon exchange amplitudes in the case of a point proton is known from the calculation in muonium and is presented in the next section.

The contributions of the fifth order in  $\alpha$  are given also by the amplitudes of particle interactions, which contain both the effects of the nuclear structure and vacuum polarization (see Fig. 7). The particle interaction operator in the coordinate representation corresponding to the diagram in Fig. 7(b) has the following form:

$$\Delta V_{str}^{vp}(r) = \frac{2}{3} \pi Z \alpha r_p^2 \frac{\alpha}{3\pi} \int_1^\infty \rho(\xi) d\xi \left[ \delta(\mathbf{r}) - \frac{m_e^2 \xi^2}{\pi r} e^{-2m_e \xi r} \right]. \quad (41)$$

Using the expression (41), we can perform analytical integration over all variables when calculating the matrix elements. For  $1S$  and  $3S$  states, the energy level shifts are equal:

$$\begin{aligned} \Delta E_{str}^{vp}(1S) &= \frac{2\alpha(Z\alpha)^4 r_p^2 \mu^3}{27\pi \sqrt{1 - b_1^2}} \left[ (6b_1^4 - 3b_1^2 + 6) \ln \left( \frac{\sqrt{1 - b_1^2} + 1}{b_1} \right) + \sqrt{1 - b_1^2} (-3\pi b_1^3 + 6b_1^2 + 1) \right], \quad (42) \\ \Delta E_{str}^{vp}(3S) &= \frac{\alpha(Z\alpha)^4 r_p^2 \mu^3}{1458\pi (1 - 9b_1^2)^{9/2}} \left\{ \sqrt{1 - 9b_1^2} [32 + 9b_1^2 (-116 + 9b_1 \{3b_1 [19 + 6b_1^2 (-5 - 414b_1^2 + 972b_1^4)] \right. \\ &\left. - 4(1 - 9b_1^2)^4 \pi)] \right\} + 3[8 + 81b_1^2 (-4 + 9b_1^2 \{10 + b_1^2 [-89 + 162b_1^2 (5 - 18b_1^2 + 36b_1^4)] \})] \ln \frac{3b_1}{1 - \sqrt{1 - 9b_1^2}} \right\}. \end{aligned} \quad (43)$$

The contribution to the energy spectrum of the same order  $\alpha(Z\alpha)^4$  is determined by the same effects in the second order of the perturbation theory [see Fig. 7(c)] by the following integral expressions:

$$\begin{aligned} \Delta E_{str,sopt}^{vp}(1S) &= \frac{2\alpha(Z\alpha)^4 \mu^3 r_p^2}{9\pi} \int_1^\infty \frac{\rho(\xi) d\xi}{(b_1 \xi + 1)^3} [2b_1^2 \xi^2 - 7b_1 \xi - 2(b_1 \xi + 1) \ln(b_1 \xi + 1) - 3], \quad (44) \\ \Delta E_{str,sopt}^{vp}(3S) &= -\frac{4\alpha(Z\alpha)^4 \mu^3 r_p^2}{81\pi} \int_1^\infty \frac{\rho(\xi) d\xi}{(2b_1 \xi + 1)^7} \left[ \ln(1 + 3b_1 \xi) 2(1 + 3b_1 \xi) (1 + 54b_1^2 \xi^2 + 243b_1^4 \xi^4) \right. \\ &\left. + [1 + 3b_1 \xi \{5 + 6b_1 \xi (1 + b_1 \xi \{28 + 3b_1 \xi \{4 + 9b_1 \xi (2 + 3b_1 \xi)\})\})] \right]. \end{aligned} \quad (45)$$

In Table I, line 16 includes the total contribution of (42) and (44) and (43) and (45). Since (42)–(45) are multiplied by  $r_p^2$  and are numerically large, they can be combined with (39) to increase the accuracy of extracting the proton charge radius in the presence of experimental data. The corrections for the two-loop vacuum polarization taking into account the structure of the proton are calculated in the same sequence. In one-photon interaction, they are shown in Fig. 9. The particle interaction operators

corresponding to these amplitudes are constructed in the integral form:

$$\Delta V_{str}^{vp-vp}(r) = \frac{2}{3} Z\alpha r_p^2 \left(\frac{\alpha}{3\pi}\right)^2 \int_1^\infty \rho(\xi) d\xi \int_1^\infty \rho(\eta) d\eta \left[ \pi \delta(\mathbf{r}) - \frac{m_e^2}{r(\xi^2 - \eta^2)} (\xi^4 e^{-2m_e \xi r} - \eta^4 e^{-2m_e \eta r}) \right], \quad (46)$$

$$\Delta V_{str}^{2-loop\ vp}(r) = \frac{4}{9} Z\alpha r_p^2 \left(\frac{\alpha}{\pi}\right)^2 \int_0^1 \frac{f(v) dv}{1-v^2} \left[ \pi \delta(\mathbf{r}) - \frac{m_e^2}{r(1-v^2)} e^{-\frac{2m_e r}{\sqrt{1-v^2}}} \right]. \quad (47)$$

In the second-order PT, the contributions of the two-loop vacuum polarization with the effect of the nuclear structure of order  $\alpha^2(Z\alpha)^4$  are shown in Fig. 10. When calculating the contribution in Fig. 10(a), it is convenient to split it into two parts when integrating over the coordinates of particles in accordance with the two terms of the potential (41). Each of them diverges upon integration over spectral parameters, but their sum is finite. Other corrections in Figs. 10(b)–10(d) are calculated in the same way, and their sum is presented in Table I (line 17). Integral expressions for these corrections before integration over spectral parameters are rather cumbersome and are not presented here (see, for example, Ref. [27]).

We also take into account in our calculation the combined sixth-order  $\alpha$  correction for the nuclear structure and vacuum polarization, which appears in two-photon exchange amplitudes as a result of the modification of the photon propagator (see Fig. 11). The corresponding particle interaction operator differs from  $V_{2\gamma}(k)$  from (40) with an additional functional factor. The integral expression for the correction of this type is [25,40,47]

$$\Delta E_{str, vp}^{2\gamma}(nS) = -\frac{2\mu^3 \alpha (Z\alpha)^5}{9\pi^2 n^3} \int_0^\infty \frac{V_{2\gamma}(k) F_{vp}(k) dk}{k^4},$$

$$F_{vp}(k) = \left[ -5k^3 + 6(k^2 - 2m_e^2) \sqrt{k^2 + 4m_e^2} \tanh^{-1} \left( \frac{k}{\sqrt{k^2 + 4m_e^2}} \right) + 12km_e^2 \right], \quad (48)$$

and its numerical value for the (3S-1S) interval is given in Table I (line 19). Other radiative corrections to the muon line [self-energy correction (se), vertex correction, and correction with an enveloping photon] with a nuclear structure of the same order  $\alpha(Z\alpha)^5$  are determined by the amplitudes in Fig. 12. Their calculation is performed for S-states in light muonic atoms in Ref. [48]. The total contribution, expressed in terms of the nuclear charge radius, is

$$\Delta E_{str, rad}^{\alpha(Z\alpha)^5}(3S - 1S) = \frac{13\mu^3 \alpha (Z\alpha)^5 r_p^2}{81} (23 - 16 \ln 2), \quad (49)$$

and numerical values are shown in line 20 of Table I.

## V. RECOIL CORRECTIONS, MUON SELF-ENERGY, AND VACUUM POLARIZATION CORRECTIONS

So far, we have considered corrections of various orders in the (3S-1S) interval, which are specific for each muonic atom. Such contributions were obtained either analytically or in the form of integral expressions and calculated numerically. In muonic atoms, expansion in terms of the characteristic parameter  $\mu Z\alpha/m_e = 1.356$  cannot be used. For the electron hydrogen atom, one can also use these expressions, replacing  $m_e \rightarrow m_\mu$ . But there is also another set of contributions that are known in analytical form and were obtained in the study of the hydrogen atom fine structure energy spectrum [19].

They can be used to estimate numerically the contributions in the case of muonic atoms. Let us briefly list the main contributions required to obtain a complete result with good accuracy [19,27–30].

There is a group of recoil corrections (the subscript *rec* is used) of various orders in  $(Z\alpha)$ , obtained in the case of a point nucleus. The recoil contribution of order  $(Z\alpha)^4 m_1^2/m_2^2$  arises when calculating the matrix elements of the Breit potential. For the hydrogen atom, such corrections are taken into account in the original formula (1). The recoil correction of order  $(Z\alpha)^5 m_1/m_2$  for S-states is determined by two-photon exchange amplitudes, in which the proton is considered as a point particle [19]:

$$\Delta E_{rec}^{(Z\alpha)^5} = \frac{\mu^3 (Z\alpha)^5}{m_1 m_2 \pi n^3} \left[ \frac{2}{3} \ln \frac{1}{Z\alpha} - \frac{8}{3} \ln k_0(n, 0) - \frac{1}{9} - \frac{7}{3} a_n - \frac{2}{m_2^2 - m_1^2} \left( m_2^2 \ln \frac{m_1}{\mu} - m_1^2 \ln \frac{m_2}{\mu} \right) \right], \quad (50)$$

where  $\ln k_0(n, 0)$  is the Bethe logarithm, which has the following values for 1S, 3S states [19]:

$$\ln k_0(1S) = 2.984128555765498, \quad \ln k_0(3S) = 2.767663612491822, \quad (51)$$

$$a_n = -2 \left[ \ln \frac{2}{n} + \left( 1 + \frac{1}{2} + \dots + \frac{1}{n} \right) + 1 - \frac{1}{2n} \right]. \quad (52)$$

The numerical value (50) for the interval (3S-1S) is large for both muonic and electron hydrogen (line 22, Table I).

The recoil correction of order  $(Z\alpha)^6 m_1/m_2$  has been studied in many works [49–51], and in Ref. [52] the corrections for the recoil of a higher order  $m_1^2(Z\alpha)^7/m_2$  are calculated. Since in our work we limited ourselves to contributions to the sixth order in

$Z\alpha$ , we use the following expression to obtain a numerical estimate (see Ref. [19]):

$$\Delta E_{rec}^{(Z\alpha)^6} (3S - 1S) = \frac{26(Z\alpha)^6 m_1^2}{27m_2} \left( \frac{7}{2} - 4 \ln 2 \right). \quad (53)$$

In the case of muonic hydrogen, the numerical value of the correction of order  $m_1^2(Z\alpha)^7/m_2$  is negligible [52].

For the energy contributions obtained from amplitudes with radiative corrections to the muon line (se), from the Dirac and Pauli form factors (ff) of the muon, there is a compact analytical representation [19]:

$$\begin{aligned} \Delta E_{se,ff}(nS) = & \frac{\alpha(Z\alpha)^4}{\pi n^3} \frac{\mu^3}{m_1^2} \left\{ \frac{4}{3} \ln \frac{m_1}{\mu(Z\alpha)^2} - \frac{4}{3} \ln k_0(n, 0) + \frac{10}{9} \right. \\ & \left. + \frac{\alpha}{\pi} \left[ -\frac{9}{4} \zeta(3) + \frac{3}{2} \pi^2 \ln 2 - \frac{10}{27} \pi^2 - \frac{2179}{648} \right] + 4\pi Z\alpha \left( \frac{427}{384} - \frac{\ln 2}{2} \right) \right\}. \end{aligned} \quad (54)$$

A discussion of higher-order contributions in  $\alpha$  can be found in Ref. [53] (see also references to other articles in this paper).

Radiative corrections with recoil of orders  $\alpha(Z\alpha)^5$  and  $(Z^2\alpha)(Z\alpha)^4$  from Table 9 [19] have the following form for  $nS$  states:

$$\begin{aligned} \Delta E_{rad-rec}(nS) = & \frac{\alpha(Z\alpha)^5 \mu^3}{m_1 m_2 n^3} \left[ 6\zeta(3) - 2\pi^2 \ln 2 + \frac{3}{4} \pi^2 - 14 \right] + \frac{\alpha(Z\alpha)^5 m_1^2}{m_2 n^3 \pi^2} \left( \frac{2\pi^2}{9} - \frac{70}{27} \right) \\ & + \frac{4(Z^2\alpha)(Z\alpha)^4 \mu^3}{\pi m_2^2 n^3} \left[ \frac{1}{3} \ln \frac{\Lambda(Z\alpha)^{-2}}{\mu} + \frac{11}{72} - \frac{1}{24} - \frac{7\pi}{32} \frac{\Lambda^2}{4m_2^2} + \frac{2}{3} \left( \frac{\Lambda^2}{4m_2^2} \right)^2 - \frac{1}{3} \ln k_0(n, 0) \right]. \end{aligned} \quad (55)$$

The formulas (54) and (55) contribute to the shift  $(3S-1S)$  (parameter  $\Lambda = \sqrt{12/r_p^2}$ ), which is shown in Table I on lines 24 and 25.

The correction for the proton structure in the energy spectrum of order  $(Z\alpha)^6$ , obtained in Ref. [28] for a muonic hydrogen-like atom with various parametrizations of the nuclear form factors, has the following form:

$$\Delta E_{str}^{(Z\alpha)^6}(nS) = \frac{2\mu(Z\alpha)^6}{3n^3} (\mu^2 F_{rel} + \mu^4 F_{nr}), \quad (56)$$

$$F_{rel} = -\langle r^2 \rangle \left[ \psi(n) + 2\gamma + \frac{9}{4n^2} - \frac{1}{n} - \frac{13}{4} + \left\langle \ln \frac{2Wr}{n} \right\rangle \right] - \frac{1}{3} \langle r^3 \rangle \left\langle \frac{1}{r} \right\rangle + I_2^{rel} + I_3^{rel}, \quad (57)$$

$$F_{nr} = \frac{2\langle r^2 \rangle}{3} \left[ \langle r^2 \rangle \left( \psi(n) + 2\gamma - \frac{1}{n} - \frac{4}{3} \right) + \left\langle r^2 \ln \frac{2Wr}{n} \right\rangle \right] + \frac{\langle r^4 \rangle}{10n^2} + \langle r^3 \rangle \langle r \rangle + \langle r^5 \rangle \left\langle \frac{1}{r} \right\rangle + I_2^{nr} + I_3^{nr}, \quad (58)$$

where the quantities  $I_{2,3}^{rel}$  and  $I_{2,3}^{nr}$ , as well as the moments of the charge distribution density, are written explicitly in Ref. [28] for various parametrizations. Based on the expressions obtained in Ref. [28], one can estimate the contributions to the shift  $(3S-1S)$  for muonic hydrogen atom (line 26 of the table).

Another numerically important contribution of the sixth order in  $\alpha$  to the shift  $(3S-1S)$  [see Fig. 13(b)] is expressed in terms of the slope of the Dirac form factor  $F_1'(0)$  and Pauli form factor  $F_2(0)$  [19], which are calculated analytically in

Ref. [54] (see line 27 of Table I):

$$\begin{aligned} \Delta E_{rad+vp} = & -\frac{7\alpha^2(Z\alpha)^4 \mu^3}{8\pi^2 m_1^2} \left[ \frac{3m_e^2}{m_1^2} - \frac{4m_e^2 \ln \frac{m_1}{m_e}}{m_1^2} + \frac{\pi^2 m_e}{4m_1} \right. \\ & \left. + \frac{4}{9} \ln^2 \frac{m_1}{m_e} - \frac{20}{27} \ln \frac{m_1}{m_e} + \frac{2\pi^2}{27} + \frac{85}{162} \right]. \end{aligned} \quad (59)$$

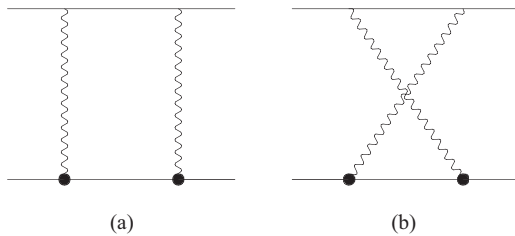


FIG. 8. Corrections to the nuclear structure of order  $(Z\alpha)^5$ . The bold point denotes the vertex operator of the proton.

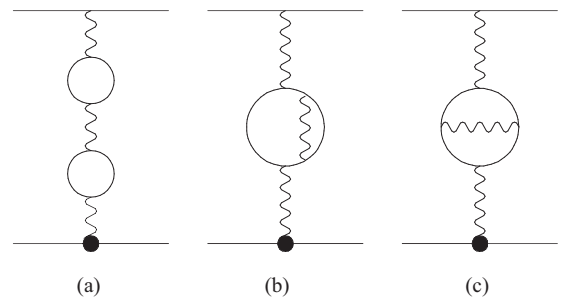


FIG. 9. Nuclear structure effects and two-loop vacuum polarization in one-photon interaction. The bold point denotes the proton vertex operator.

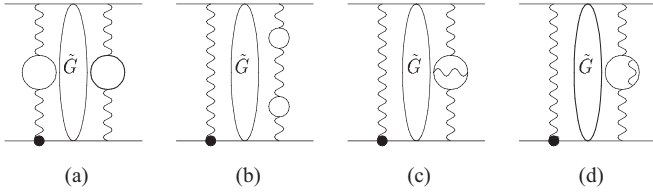


FIG. 10. Nuclear structure and two-loop vacuum polarization effects in the second order of perturbation theory. The bold point denotes the proton vertex operator.  $\tilde{G}$  is the reduced Coulomb Green's function.

In the case of electron hydrogen, a numerically large contribution is giving by radiative corrections of order  $\alpha(Z\alpha)^6$  (see Table 5 in Ref. [19]). We have included it in our Table I for muonic hydrogen in line 31.

To estimate the contribution of the muon self-energy (mse) taking into account the vacuum polarization, the following expression was obtained in the logarithmic approximation in Ref. [30]:

$$\Delta E_{mse}^{vp}(n) = \frac{\alpha}{3\pi m_1^2} \ln \frac{m_1}{\mu(Z\alpha)^2} \left[ \langle \psi_n | \Delta \cdot \Delta V_{vp}^C | \psi_n \rangle + 2 \langle \psi_n | \Delta V_{vp}^C \tilde{G} \Delta \left( -\frac{Z\alpha}{r} \right) | \psi_n \rangle \right]. \quad (60)$$

Assuming as in calculating relativistic corrections  $\mathbf{p}^2 = 2\mu(H + Z\alpha/r)$  and calculating numerous matrix elements in (60), we obtain a correction in the interval (3S-1S) (line 28).

Taking into account the accuracy of the calculation, we have included in the complete result for the shift (3S-1S) the contribution of hadronic vacuum polarization (hvp), which was investigated in Refs. [55–57] in the case of muonic hydrogen.

Figure 14 shows four amplitudes of light-by-light scattering. The amplitude in Fig. 14(a) denotes the contribution known as the Wichmann-Kroll correction (see the approximation potential in Ref. [19]). It is shown in Table I on line 4. In Refs. [58,59] it was shown that the contribution of the amplitude in Fig. 14 differs from the Wichmann-Kroll contribution by the factor  $1/Z^2$ . The interaction potential in Figs. 14(c) and 14(d) was obtained in Ref. [58] using the Padé approximation in a convenient form for numerical calculations of corrections in the energy spectrum (the coefficients  $s_i$ ,  $t_i$  are written in Ref. [58]; index  $ll$  corresponds to the abbreviation

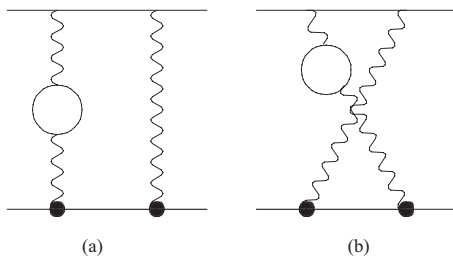


FIG. 11. Nuclear structure and vacuum polarization effects in two-photon exchange diagrams. The bold point denotes the proton vertex operator.

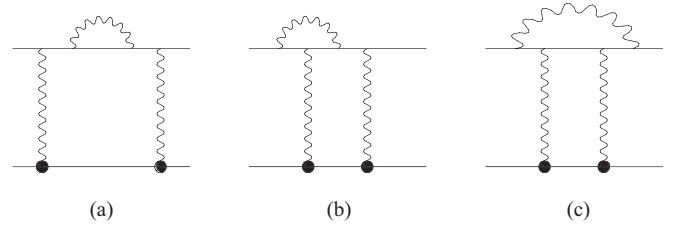


FIG. 12. Two-photon exchange amplitudes with radiative corrections to the muon line, contributing to the order  $\alpha(Z\alpha)^5$ . The bold point shows the proton vertex operator.

light-by-light):

$$\Delta V^{ll}(r) = -\frac{\alpha^2(Z\alpha)^2}{r} \frac{(s_0 + s_1x + s_2x^2)}{(t_0 + t_1x + t_2x^2 + t_3x^3 + t_4x^4 + t_5x^5)}, \quad (61)$$

$$x = m_e r.$$

Numerical value of the corresponding correction [see line 5, in which the total contribution of the amplitudes in Figs. 14(b)–14(d) is written out] is important for refining the complete result.

There is one more effect of light-by-light scattering, which leads to the appearance of an effective one-meson interaction between a muon and a proton (scalar, pseudoscalar, axial-vector, and tensor). Studies of such a mechanism in Refs. [60–62] have shown that in muonic hydrogen, the exchange of a scalar meson gives a significant shift of the S-energy levels  $\Delta E(3S - 1S) = -0.1059$  meV. Therefore, it was also included in the final Table I for muonic hydrogen.

## VI. NUMERICAL RESULTS AND CONCLUSION

In this work, we continue our studies [25–27,40] of low-lying energy levels of muonic hydrogen, which have been intensively studied in recent years experimentally and theoretically. The (3S-1S) transition was chosen as the energy interval for a precision calculation, the measurement accuracy of which in the case of electron hydrogen is very high [15]. Various potentially important interactions in muonic hydrogen are analyzed and their contribution to the structure of S-states is calculated within the framework of the quasipotential method in quantum electrodynamics. We have calculated the energy interval (3S-1S) in muonic hydrogen taking into account corrections of the fifth and sixth orders in  $\alpha$  and

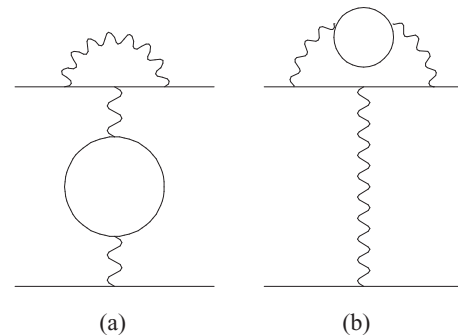


FIG. 13. Radiative corrections with vacuum polarization effects.



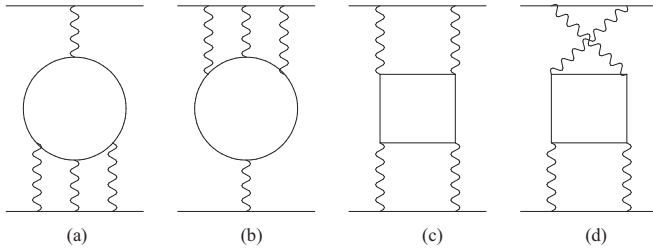


FIG. 14. The amplitudes of light-by-light scattering.

taking into account the effects of recoil and the structure of the proton. We also used numerous results of calculations of other corrections performed by different authors and took into account numerically important effects of higher order in  $\alpha$ .

The interest in the transitions between the  $S$ -energy levels in the hydrogen atom is due to the fact that the study of such transitions opens up yet another possibility of refining the value of the charge radius of the nucleus (proton). As noted earlier, experiment [15] is quite consistent with the CODATA result for the proton charge radius, unlike all other new experiments with both muonic and electronic systems. In this regard, it was useful to calculate the energy interval ( $3S$ - $1S$ ) in muonic hydrogen, bearing in mind the possible perspective of its measurement in the future.

In recent years, different groups have performed calculations of new corrections in the fine and hyperfine structure of the spectrum of muonic atoms, including for the  $S$ -energy levels. Since the number of such papers is significant, references to many other papers can be found in the review papers [9,10,19,29,63]. Although these works did not directly calculate the energy interval ( $3S$ - $1S$ ), some comparison with the results obtained earlier can be made. Most of the corrections we calculated for vacuum polarization (Uehling, Källén-Sabry, Wichmann-Kroll corrections) are in good agreement with previous calculations [9,10,29,64,65], but in this work these corrections are not presented in summary form, but in more detail. Our calculations of three-loop VP effects in one-photon interaction are based on the Kinoshita-Nio interpolation formula (eight diagrams in Fig. 2), which gives the known result for the Lamb shift from Ref. [32]. For the interval ( $3S$ - $1S$ ), this contribution was obtained, as well as the contribution of the three-loop polarization operator with two fermionic cycles in Fig. 3, calculated on the basis of the analytical formula for the polarization operator from Refs. [38,39]. We have worked out in detail the calculation of combined corrections for the vacuum polarization with relativistic effects. We have written the corresponding potentials and matrix elements in the first and second orders of the perturbation theory. We obtain an expression for the reduced Coulomb Green's function of the  $3S$ -state with two nonzero arguments, which is necessary for calculating corrections in the second and third orders of the perturbation theory. General expressions for calculating the effects of a three-loop VP in the third order of perturbation theory agree with Refs. [64,65], and numerical results themselves are unique to this study to the best of our knowledge,

as well as are numerous corrections for the proton structure. Note that to calculate the effects of light-by-light scattering, we use the formula for the potential obtained in Ref. [58]. The calculation of corrections in Sec. V is based on well-known analytical expressions (see Ref. [19]), and the results are presented in detail in Table I.

The calculated contributions are presented in the work in the form of analytical formulas, integral expressions that can be integrated numerically, as well as in numerical form in Table I. Most of the results for muonic hydrogen in Table I are presented with an accuracy of four digits after the decimal point in meV, since the errors in their determination due to the errors of fundamental physical constants are much smaller. But there are contributions to the proton structure, which are determined by the strong interaction and have been obtained so far with a significant error. The total theoretical result for the energy interval ( $3S$ - $1S$ ) in muonic hydrogen has the form  $\Delta E(\mu p) = 2\,249\,398.5478$  meV. The error in calculating the main contribution (see line 1 in Table I) due to the uncertainties of the fundamental physical constants does not exceed 0.0015 meV. A rough estimate of the contribution of order  $m\alpha^7$  gives a value 0.0001 meV. It is impossible to calculate the proton form factors with the required accuracy in quantum chromodynamics, and the use of experimental data on the form factors obviously gives its part of the error. Our estimate of such an error in calculating the two-photon exchange amplitudes is shown directly in Table I (line 18). An estimate of the contribution to the proton polarizability is taken from the work [66]. The total error in calculating the proton polarizability contribution and nuclear structure correction of order  $(Z\alpha)^5$  0.025 meV leads to an error in determining the charge radius of the proton 0.00035 fm. The theoretical error in the calculation of the interval ( $3S$ - $1S$ ) connected with the calculation of the QED corrections is, according to our estimates, about 0.005 meV. The largest contribution to the structure of the proton is connected with a correction of order  $(Z\alpha)^4$  (line 15 of Table I). Its numerical value is obtained with the proton charge radius from [9]. If we do not fix numerical value of the correction (39), then the total result from Table I can be presented as

$$\Delta E^{\text{tot}}(3S-1S) = 2\,249\,426.8578(250) - 40.039631(3) r_p^2 \text{ meV}, \quad (62)$$

where the value of the charge radius  $r_p$  is taken in fm. Thus, a precision measurement of the frequency of the ( $3S$ - $1S$ ) transition in muonic hydrogen can give a more exact value of the proton's charge radius. So, for example, measuring the ( $3S$ - $1S$ ) shift in muonic hydrogen with a relative error (1–3) ppb together with an improvement in the accuracy of calculating the effect of nuclear polarizability and a correction to the structure of the nucleus of order  $(Z\alpha)^5$  will reduce the error in determining the proton charge radius to 0.0001 fm.

#### ACKNOWLEDGMENT

This work was supported by the Russian Science Foundation (Grant No. 18-12-00128).



- [1] R. J. Hill, *EPJ Web Conf.* **137**, 01023 (2017).
- [2] G. Paz, [arXiv:1909.08108](https://arxiv.org/abs/1909.08108) [hep-ph].
- [3] M. Horbatsch, E. A. Hessels, and A. Pineda, *Phys. Rev. C* **95**, 035203 (2017).
- [4] J. C. Bernauer, *EPJ Web Conf.* **234**, 01001 (2020).
- [5] C. E. Carlson, *Prog. Part. Nucl. Phys.* **82**, 59 (2015).
- [6] S. G. Karshenboim, V. G. Ivanov, and S. I. Eidelman, *Phys. Part. Nucl. Lett.* **16**, 514 (2019).
- [7] R. Pohl, A. Antognini, F. Nez, F. D. Amaro, F. Biraben, J. M. R. Cardoso, D. S. Covita, A. Dax, S. Dhawan, L. M. P. Fernandes, A. Giesen *et al.*, *Nature (London)* **466**, 213 (2010).
- [8] A. Antognini, F. Nez, K. Schuhmann, F. D. Amaro, F. Biraben, J. M. R. Cardoso, D. S. Covita, A. Dax, S. Dhawan, M. Diepold *et al.*, *Science* **339**, 417 (2013).
- [9] A. Antognini, F. Kottmann, F. Biraben, P. Indelicato, F. Nez, and R. Pohl, *Ann. Phys.* **331**, 127 (2013).
- [10] R. Pohl, F. Nez, L. M. P. Fernandes, F. D. Amaro, F. Biraben, J. M. R. Cardoso, D. S. Covita, A. Dax, S. Dhawan, M. Diepold *et al.*, *Science* **353**, 669 (2016).
- [11] A. Beyer, L. Maisenbacher, A. Matveev, R. Pohl, K. Khabarova, A. Grinin, T. Lamour, D. C. Yost, Th. W. Hänsch, N. Kolachevsky, and Th. Udem, *Science* **358**, 79 (2017).
- [12] W. Xiong, A. Gasparian, H. Gao, D. Dutta, M. Khandaker, N. Liyanage, E. Pasyuk, C. Peng, X. Bai, L. Ye *et al.*, *Nature (London)* **575**, 147 (2019).
- [13] N. Bezginov, T. Valdez, M. Horbatsch, A. Marsman, A. C. Vutha, and E. A. Hessels, *Science* **365**, 1007 (2019).
- [14] R. Gilman, E. J. Downie, G. Ron, S. Strauch, A. Afanasev, A. Akmal, J. Arrington, H. Atac, C. Ayerbe-Gayoso, F. Benmokhtar *et al.* (MUSE Collaboration), [arXiv:1709.09753](https://arxiv.org/abs/1709.09753) [physics.ins-det].
- [15] H. Fleurbaey, S. Galtier, S. Thomas, M. Bonnaud, L. Julien, F. Biraben, F. Nez, M. Abgrall, and J. Guéna, *Phys. Rev. Lett.* **120**, 183001 (2018).
- [16] P. J. Mohr, D. B. Newell, and B. N. Taylor, *Rev. Mod. Phys.* **88**, 035009 (2016).
- [17] C. G. Parthey, A. Matveev, J. Alnis, B. Bernhardt, A. Beyer, R. Holzwarth, A. Maistrou, R. Pohl, K. Predehl, T. Udem *et al.*, *Phys. Rev. Lett.* **107**, 203001 (2011).
- [18] I. Fan, C.-Y. Chang, L.-B. Wang, S. L. Cornish, J.-T. Shy, and Y.-W. Liu, *Phys. Rev. A* **89**, 032513 (2014).
- [19] M. I. Eides, H. Grotch, and V. A. Shelyuto, *Phys. Rep.* **342**, 62 (2001); *Theory of Light Hydrogenic Bound States* (Springer, Berlin, 2007).
- [20] P. Crivelli, *Hyperfine Interact.* **239**, 49 (2018).
- [21] R. K. Altmann, S. Galtier, L. S. Dreissen, and K. S. E. Eikema, *Phys. Rev. Lett.* **117**, 173201 (2016).
- [22] V. A. Yerokhin, K. Pachucki, and V. Patkos, *Ann. Phys.* **531**, 00324 (2018).
- [23] R. Pohl, H. Daniel, F. J. Hartmann, P. Hauser, F. Kottmann, V. E. Markushin, M. Muhlbauer, C. Petitjean, W. Schott, D. Taqqu *et al.*, *Phys. Rev. Lett.* **97**, 193402 (2006).
- [24] V. P. Popov and V. N. Pomerantsev, [arXiv:0809.0742](https://arxiv.org/abs/0809.0742) [nucl-th].
- [25] A. P. Martynenko, *J. Exp. Theor. Phys.* **101**, 1021 (2005).
- [26] A. A. Krutov, A. P. Martynenko, G. A. Martynenko, and R. N. Faustov, *J. Exp. Theor. Phys.* **120**, 73 (2015).
- [27] A. E. Dorokhov, A. P. Martynenko, F. A. Martynenko, and R. N. Faustov, *J. Exp. Theor. Phys.* **129**, 956 (2019).
- [28] J. L. Friar, *Ann. Phys.* **122**, 151 (1979).
- [29] E. Borie, *Ann. Phys.* **327**, 733 (2012).
- [30] K. Pachucki, *Phys. Rev. A* **54**, 1994 (1996).
- [31] G. Källén and A. Sabry, *Mat. Fys. Medd. Dan. Vid. Selesk.* **29**, 1 (1955), in *Portrait of Gunnar Källén*, edited by C. Jarlskog (Springer, Cham, 2014), p. 555.
- [32] T. Kinoshita and M. Nio, *Phys. Rev. Lett.* **82**, 3240 (1999).
- [33] T. Kinoshita and M. Nio, *Phys. Rev. D* **60**, 053008 (1999).
- [34] T. Kinoshita and W. B. Lindquist, *Phys. Rev. D* **27**, 853 (1983).
- [35] P. A. Baikov and D. J. Broadhurst, in *New Computing Techniques in Physics Research IV*, edited by B. Denby and D. Perrei-Gallix (World Scientific, Singapore, 1995), p. 167.
- [36] R. N. Faustov, A. L. Kataev, S. A. Larin, and V. V. Starshenko, *Phys. Lett. B* **254**, 241 (1991).
- [37] D. J. Broadhurst, A. L. Kataev, and O. V. Tarasov, *Phys. Lett. B* **298**, 445 (1993).
- [38] A. H. Hoang, J. H. Kühn, and T. Teubner, *Nucl. Phys. B* **452**, 173 (1995).
- [39] K. G. Chetyrkin, A. H. Hoang, J. H. Kühn, M. Steinhauser and T. Teubner, *Phys. Lett. B* **384**, 233 (1996).
- [40] A. P. Martynenko, *Phys. Rev. A* **76**, 012505 (2007).
- [41] A. A. Krutov, A. P. Martynenko, F. A. Martynenko, and O. S. Sukhorukova, *Phys. Rev. A* **94**, 062505 (2016).
- [42] H. F. Hameka, *J. Chem. Phys.* **47**, 2728 (1967).
- [43] M. G. Veselov and L. N. Labzovsky, *Atomic Theory: Electron Shell Structure* (Nauka, Moscow, 1986).
- [44] V. G. Ivanov and S. G. Karshenboim, *J. Exp. Theor. Phys.* **82**, 656 (1996).
- [45] V. G. Ivanov, E. Yu. Korzinin, and S. G. Karshenboim, *Phys. Rev. D* **80**, 027702 (2009).
- [46] J. J. Kelly, *Phys. Rev. C* **70**, 068202 (2004).
- [47] A. E. Dorokhov, A. A. Krutov, A. P. Martynenko, F. A. Martynenko, and O. S. Sukhorukova, *Phys. Rev. A* **98**, 042501 (2018).
- [48] R. N. Faustov, A. P. Martynenko, F. A. Martynenko, and V. V. Sorokin, *Phys. Lett. B* **775**, 79 (2017).
- [49] M. I. Eides and H. Grotch, *Phys. Rev. A* **55**, 3351 (1997).
- [50] K. Pachucki and H. Grotch, *Phys. Rev. A* **51**, 1854 (1995).
- [51] V. M. Shabaev, *Theor. Math. Phys.* **63**, 588 (1985).
- [52] V. A. Yerokhin and V. M. Shabaev, *Phys. Rev. Lett.* **115**, 233002 (2015).
- [53] V. A. Yerokhin and V. M. Shabaev, *J. Phys. Chem. Ref. Data* **44**, 033103 (2015).
- [54] R. Barbieri, M. Caffo, and E. Remiddi, *Nuovo Cimento Lett.* **7**, 60 (1973).
- [55] E. Borie, *Z. Phys. A* **302**, 187 (1981).
- [56] J. L. Friar, J. Martorell, and D. W. L. Sprung, *Phys. Rev. A* **59**, 4061 (1999).
- [57] A. P. Martynenko and R. N. Faustov, *Phys. Atom. Nucl.* **64**, 1282 (2001).
- [58] E. Y. Korzinin, V. A. Shelyuto, V. G. Ivanov, R. Szafron, and S. G. Karshenboim, *Phys. Rev. A* **98**, 062519 (2018).
- [59] S. G. Karshenboim, E. Yu. Korzinin, V. G. Ivanov, and V. A. Shelyuto, *JETP Lett.* **92**, 8 (2010).
- [60] A. E. Dorokhov, A. P. Martynenko, F. A. Martynenko, and A. E. Radzhabov, *EPJ Web Conf.* **222**, 03010 (2019).
- [61] A. E. Dorokhov, N. I. Kochelev, A. P. Martynenko, F. A. Martynenko, and R. N. Faustov, *Phys. Part. Nucl. Lett.* **14**, 857 (2017).

- [62] A. E. Dorokhov, N. I. Kochelev, A. P. Martynenko, F. A. Martynenko, and A. E. Radzhabov, *Phys. Lett. B* **776**, 105 (2018).
- [63] B. Franke, J. J. Krauth, A. Antognini, M. Diepold, F. Kottmann, and R. Pohl, *EPJ D* **71**, 341 (2017).
- [64] E. Y. Korzinin, V. A. Shelyuto, V. G. Ivanov, and S. G. Karshenboim, *Phys. Rev. A* **97**, 012514 (2018).
- [65] S. G. Karshenboim, V. G. Ivanov, E. Y. Korzinin, and V. A. Shelyuto, *Phys. Rev. A* **81**, 060501(R) (2010).
- [66] A. P. Martynenko, *Phys. Atom. Nucl.* **69**, 1309 (2006).